ACS APPLIED MATERIALS & INTERFACES

Research Article

www.acsami.org

Facile Preparation of Porous Carbon Nanosheets without Template and Their Excellent Electrocatalytic Property

Yichen Wang[†,‡] and Xiue Jiang*[,†]

[†]State Key Laboratory of Electroanalytical Chemistry, Changchun Institute of Applied Chemistry, Chinese Academy of Science, Changchun 130022, China

[‡]University of Chinese Academy of Sciences, Beijing 100049, China

ABSTRACT: A novel porous carbon nanosheet was successfully fabricated by a one-step annealing process with folic acid as the carbon source in the absence of any other reagents or templates. The product exhibited a large specific surface area and good porosity. Meanwhile, the carbon nanosheets as a metal-free catalyst showed a high electrocatalytic activity toward the oxygen reduction reaction (ORR) in alkaline solution, including superior onset and reduction potentials as well as a nearly four-electron pathway.

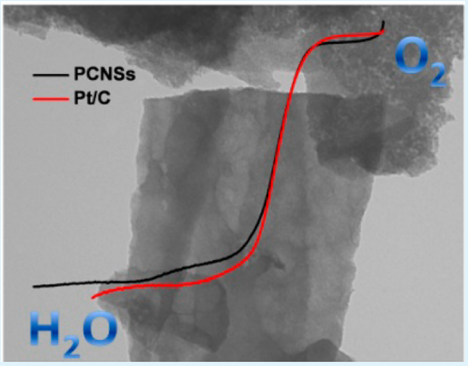

KEYWORDS: *carbon nanosheets, folic acid, oxygen reduction reaction, four-electron pathway, rotating ring-disk electrode*

1. INTRODUCTION

During the past few years, direct liquid fuel cells have drawn considerable attention because of their high efficiency and low environmental pollution.[1] One of the most crucial components of these fuel cells is the performance of the electrocatalysts for the cathodic oxygen reduction reaction (ORR), which can significantly limit the performance of the cells.[2,3] Although platinum-based materials have been regarded as the best catalysts for the ORR, the drawbacks of Pt, including their high cost, resource limitation, sluggish ORR process, and methanol and CO deactivation, extensively restrict their application in the field of fuel cells.[1,4,5] Over recent decades, many researchers have devoted themselves to developing novel catalysts to reduce or replace Pt-based catalysts in fuel cells, and some new improvements have been made, such as Pt-based alloys,[6,7] silver,[8] gold,[9] transition metals,[10,11] and heteroatom-doped metal-free catalysts. Among these materials, heteroatom-doped carbon nanomaterials have been demonstrated to be a promising metal-free electrocatalyst because of their high ORR activities, relatively low cost, and excellent tolerance toward methanol.[12−14] Doping nitrogen to carbon structures has proved to be an effective strategy to synthesize superior heteroatom-doped catalysts because the incorporation of nitrogen atoms in the carbon architecture may change the interaction between adjacent carbons and electrons.[4,12,13,15−17] Other carbon materials doped by single (such as sulfur, boron, phosphorus, and selenium) or dual heteroatoms (sulfur/nitrogen, boron/nitrogen) have also been designed to catalyze oxygen reduction.[14,18−21] Although great progress has been made, there are still some challenges in the development of electrocatalysts.

Currently, numerous efforts have been made to develop a simple and green method for preparing nanomaterials, especially the preparation protocols that use as few reagents as possible. Some groups have reported new methods to synthesize novel metal nanoparticles on the surface of graphene oxide or graphene in the absence of any additional protecting molecules or reductants.[9,21] In the field of preparing a metal-free carbon electrocatalyst, there are two major strategies reported in recent years. One strategy is to introduce the heteroatoms to the framework of a carbon nanotube or graphene,[13,21−23] and the other is to use carbon-rich molecules containing heteroatoms as carbon sources to synthesize carbon nanomaterials in the presence of templates.[12,15,24] However, the prepreparation of a carbon nanotube and graphene or the introduction of templates renders the overall procedures complicated. Besides this, the toxicity of some reagents further contradicts the attractiveness of these approaches. Therefore, developing facile and nonpolluting strategies are highly desirable.

Here, we report a one-step procedure for preparing porous carbon nanosheets (PCNSs) based on a facile and eco-friendly strategy that employs folic acid (FA) as a carbon precursor to synthesize carbon nanomaterial via an annealing method for the first time. The small molecules of the carbon source can grow

Received: July 4, 2013
Accepted: November 5, 2013
Published: November 5, 2013

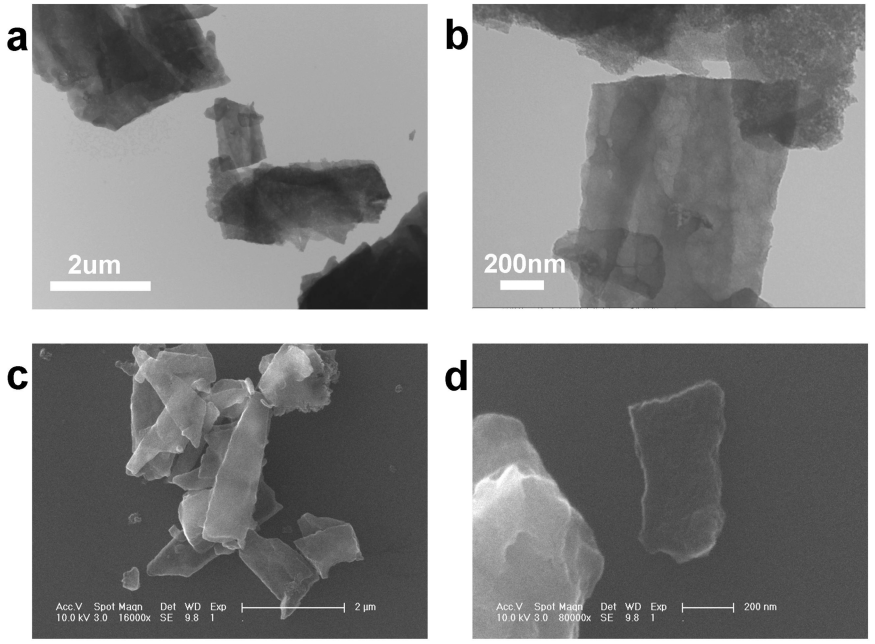

Figure 1. (a, b) TEM and (c, d) SEM images of the as-prepared PCNSs.

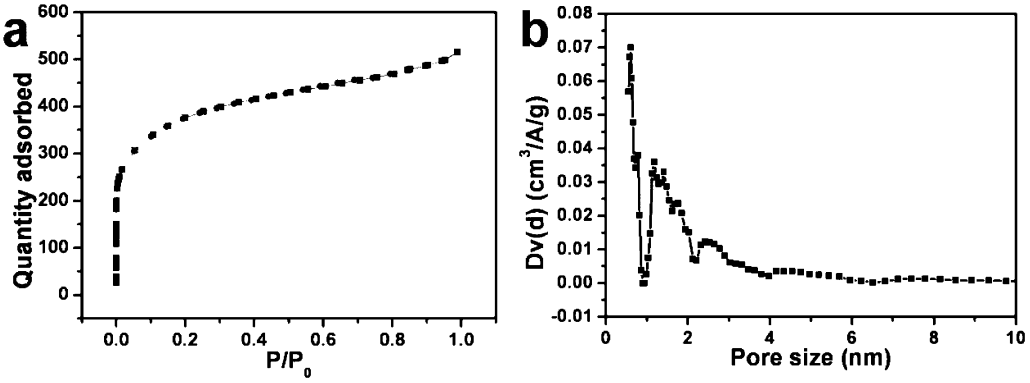

Figure 2. (a) Nitrogen adsorption–desorption isotherm and (b) pore-size distribution of PCNSs.

into nanostructures through a simple annealing process without adding additional agents or templates. Most importantly, the as-prepared metal-free nanomaterials exhibit enhanced electrocatalytic activity and stability toward the ORR in alkaline solution.

2. EXPERIMENTAL SECTION

2.1. Synthesis of PCNSs. PCNSs were prepared through a high-temperature annealing process. In a typical preparation experiment, 100 mg of FA was added to a combustion boat, and the combustion boat was then transferred into a tube furnace and heated at 900 °C for a period of 6 h under a N_2 atmosphere at a rate of 2.5 °C min^{-1}. The as-prepared product was crushed to powder and dispersed in a mixture of ethanol and Nafion (9:1), which was then subjected to ultrasonication for 3 h before further use.

2.2. Measurements. Transmission electron microscopy (TEM) and scanning electron microscopy (SEM) measurements of the as-prepared sample were conducted on HITACHI H-8100EM (Hitachi, Tokyo, Japan) and FEI/Philips XL30 ESEM FEG field-emission scanning electron microscopes. Nitrogen adsorption isotherms were measured with a Quadrachrome Autosorb automated gas sorption system. The surface area was calculated using the Brunauer–Emmett–Teller (BET) method based on adsorption data. The pore-size distribution was determined via a nonlocal density functional theory (NLDFT) method using nitrogen adsorption data. The Raman spectrum was acquired with a JY-HR800 spectrometer with a radiation of 514.5 nm. X-ray photoelectron spectroscopy (XPS) measurements were performed on an ESCALAB 250 X-ray photoelectron spectrometer with a monochromated X-ray source (Al Kα $h\nu$ = 1486.6 eV). The elemental analysis measurement was performed on a VarioEL elemental analysis system. Cyclic voltammetry (CV) experiments were carried out using a computer-controlled CHI750D electrochemical analyzer (CH Instruments, Inc., Shanghai) in a homemade three-electrode electrochemical cell. The rotating ring-disk voltammograms were collected on a PINE Research Instrumentation AFMSRCE2900 ring-disk electrode system. A conventional three-electrode system was used in all of the electrochemical measurements. A Ag/AgCl (in saturated KCl) and Pt coils were used as the reference and counter electrode, respectively, and a PCNSs-modified glassy carbon electrode (PCNSs/GCE) was used as the working electrode. The PCNSs/GCE was prepared by a simple casting method. Prior to surface coating, the GCE was polished with 1.0 and 0.3 μm alumina powder, respectively, and rinsed with doubly distilled water followed by sonication in ethanol and doubly distilled water successively. Then, the electrode was dried in a stream of N_2. Afterwards, 2 μL of the PCNSs solution (4 mg/mL) was dropped onto the surface of the pretreated GCE (d = 3 mm) for CV measurements, and 8 μL of the PCNSs solution was dropped onto the 5.6 mm rotating ring-disk electrode (RRDE) for RRDE experiments. The electrodes were left to

dry at room temperature. Similarly, commercial Pt/C (20 wt % platinum on carbon black) modified GCE (Pt/C/GCE) prepared in the same amount (4 mg/mL, 2 μL for CV measurements, 8 μL for RRDE experiments) was also studied for comparison. N_2- or O_2-saturated electrolyte was prepared by blowing the electrolyte solution with ultrahigh purity N_2 or O_2 for 15 min and then sealing the solution with N_2 and O_2 atmospheres, respectively, during the experimental procedure. All electrochemical experiments were performed at room temperature.

3. RESULTS AND DISCUSSION

For the preparation of PCNSs, FA was annealed at 900 °C for 6 h under a N_2 atmosphere. A black powder was acquired after the process. The as-prepared material was investigated first by TEM. Figure 1a shows the low-magnification TEM picture of the PCNSs. The morphology of the product is quasi-rectangular nanosheets ranging in size from ∼900 nm to several micrometers, supported by the SEM photos (Figure 1c,d). Loose structures were also observed in the high-magnification TEM picture (Figure 1b), which implies the possibility of the existence of pore structures. To investigate the porosity of the as-prepared PCNSs, we employed the nitrogen adsorption technique. The nitrogen adsorption−desorption isotherm of PCNSs shows a type-I isotherm without any obvious hysteresis loop (Figure 2a). The BET surface area is 1358 $m^2\ g^{-1}$ based on the nitrogen adsorption analysis. This result indicates that the PCNSs possess a large specific surface area, which is larger than some reported porous carbon nanomaterials prepared with templates or some complicated processes.[24−27] Figure 2b shows the pore-size distribution of the PCNSs calculated by the NLDFT method. The featureless line is in the range of 4−10 nm, and the line starts to rise from 4 nm, indicating that the pore size is less than 4 nm. The average pore size obtained from the pore-size data is 2.353 nm. According to the pore-size recommendations of IUPAC, the width of a mesopore is from 2 to 50 nm, and the width of a micropore is less than 2 nm. Therefore, these results demonstrate the existence of a large number of micropores and mesopores on the PCNSs.

Raman spectroscopy has historically played a significant role in the research of graphitic materials, especially carbon nanostructures.[28] Figure 3 shows the Raman spectrum of the PCNSs. Obviously, there are two peaks at about 1340 and 1590 cm^{-1}, corresponding to the D and G bands, respectively. The peak of the G band, which has been assigned to the E_{2g} phonon of C sp^2 atoms,[28,29] shows the graphitization of the as-prepared sample through the high-temperature process. Meanwhile, the peak of D band, which represents a breathing mode of κ-point phonons of A_{1g} symmetry, is always an indication of disorder. Its appearance implies the existence of defect on the PCNSs.

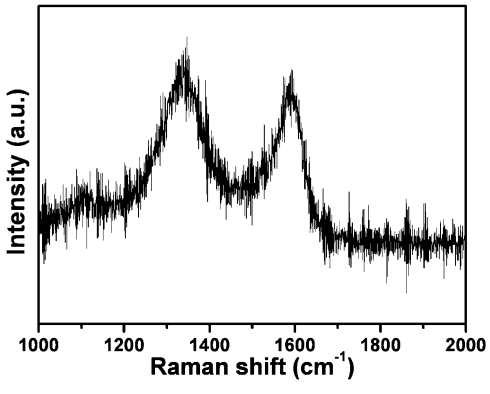

Figure 3. Raman spectrum of the PCNSs.

XPS measurement was performed to probe the chemical composition of the PCNSs and the chemical status of these elements. Figure 4a shows the survey scan spectrum of the PCNSs with apparent C 1s and O 1s peaks. Figure 4b shows the high-resolution spectrum of C 1s. It can be deconvoluted into four peaks at 284.5, 285.2, 286.6, and 289.1 eV, corresponding to sp^2 carbon, sp^3 carbon, C−O, and O−C═O, respectively.[30,31] The obvious presence of sp^3 carbon indicates a large amount of defects on the sample, which is in agreement with the information from the Raman result. Interestingly, although an FA molecule has many nitrogen atoms, the PCNSs prepared from the FA show only a weak signal for the N, which can be resolved only at the high-resolution spectrum of N 1s (Figure 4c). Elemental analysis was further employed to determine the content of N. The percentage of the N element in the material is 1.55 wt %, which also confirms the property of N-doped material for PCNSs.

Annealed carbon nanomaterials often have the capability to catalyze the ORR.[12,15,24] On the basis of this fact, we expect PCNSs to possess excellent electrocatalytic activity. The catalytic performance of the PCNSs toward the ORR was first investigated by CV measurement. Figure 5a shows the cyclic voltammograms of O_2 reduction at the bare GCE and the PCNSs/GCE in a 0.1 M KOH solution at a scan rate of 50 mV s^{-1}. There is no obvious peak in the potential window ranging from 0.15 to −1.0 V at the PCNSs/GCE in the N_2-saturated solution (black line). However, a distinct reduction peak appears at the potential of −0.21 V with the onset potential at −0.02 V in the O_2-saturated solution (red line), revealing that the PCNSs have excellent electrocatalytic activity toward the ORR. This result is also confirmed by the comparison between the PCNSs/GCE and the bare GCE in the N_2- or O_2-saturated 0.1 M KOH solution. The onset and reduction potentials of ORR at the bare GCE are −0.21 and −0.40 V, respectively, in the O_2-saturated electrolyte (pink line) in comparison with in the N_2-saturated electrolyte solution (green line). When 3 M methanol was added to the solution, the current of the oxygen reduction was negligibly affected at the PCNSs/GCE (blue line). To compare the electrocatalytic activity of the PCNSs, we researched the ORR catalyzed by commercial Pt/C catalyst. Figure 5b shows the cyclic voltammograms of the ORR recorded at the Pt/C/GCE under the same test conditions. The onset and reduction potentials are around 0.01 and −0.15 V, respectively, in the O_2-saturated (red line) 0.1 M KOH solutions in comparison with in the N_2-saturated (black line) KOH solution. Nevertheless, the ORR at the Pt/C/GCE was significantly interfered with in the presence of 3 M methanol, resulting in the disappearance of the ORR peak and the appearance of the methanol oxidation peak (blue line). These results suggest that the PCNSs possess excellent tolerance to methanol. In addition, the reduction potential and the onset potential of the ORR at the PCNSs/GCE exhibit only a 0.06 and 0.03 V negative shift, respectively, compared to those at Pt/C/GCE. Compared with the reported results,[9,13,32] it is competitive. Because the onset potential is an important parameter to evaluate the activity of electrocatalysts,[33] the as-prepared material is a promising catalyst.

To gain further insight into the electrocatalytic activity of the PCNSs/GCE toward ORR, we investigated the reaction

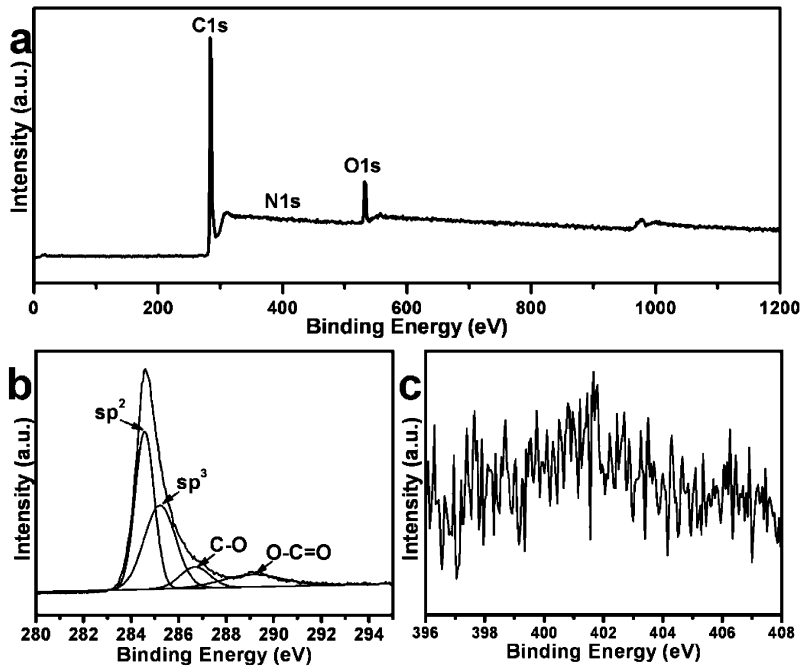

Figure 4. (a) XPS survey scan and high-resolution spectra of (b) C 1s and (c) N 1s.

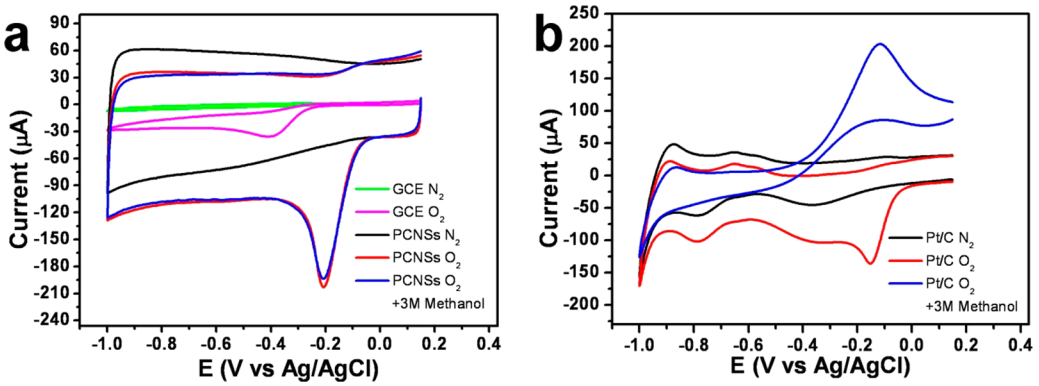

Figure 5. Cyclic voltammograms of (a) bare GCE and PCNSs/GCE and (b) Pt/C/GCE in N_2- or O_2-saturated 0.1 M KOH or O_2-saturated 0.1 M KOH containing 3 M CH_3OH solutions at a scan rate of 50 mV s^{-1}.

kinetics by RRDE. Figure 6a,b shows the RRDE results at the PCNSs/GCE and the Pt/C/GCE in the O_2-saturated 0.1 M KOH solution at the rotation rate of 1600 rpm. The ring current was measured to evaluate the amount of generated hydrogen peroxide ions, which were detected by a Pt ring electrode at a potential of 0.50 V.[4] A small ring current generated during the ORR process indicates good catalytic performance of the PCNSs. The electron-transfer number per oxygen molecule involved in the ORR was determined using the following equation[4,9]

$$n = \frac{4I_d}{I_d + \frac{I_r}{N}} \quad (1)$$

where N is the collection efficiency of the ring electrode, which was determined to be 0.37 for our electrode, I_d is the Faradic disk current, and I_r is the Faradic ring current. Figure 6c shows the electron-transfer number of the ORR at different potentials. Within the potential range from −0.3 to −0.7 V, the n value is estimated to be 3.49−3.67 at PCNSs/GCE. In contrast, the electron-transfer number of the ORR at the Pt/C/GCE is estimated to be 3.88−3.97 within the same potential range, so there is not a wide difference between the PCNSs and Pt/C (Figure 6c). These results indicate that the ORR at the PCNSs/GCE is nearly via a four-electron pathway, as is the case for many reported metal-free carbon materials doped by nitrogen.[4,12,13,24]

Compared with the electron-transfer numbers of reported N-doped carbon materials, which are in the range of 3.2−3.9,[12,13,15,34,35] the performance of the PCNSs is comparable. Most importantly, the values of electron-transfer number of the ORR at the PCNSs/GCE are similar at different potentials from −0.3 to −0.7 V, whereas the value varies with potential at some N-doped carbon-materials-modified electrodes.[5,34] This phenomenon indicates that the PCNSs possess high catalytic activity toward the ORR, which is similar to the response of Pt/C to a change of potentials (Figure 6c). In addition, the limiting current density at the PCNSs/GCE (4.6 mA cm^{-2} at −0.8 V) is similar to that at the Pt/C/GCE (4.9 mA cm^{-2} at −0.8 V) when the same amount of catalyst was used. Some researchers have reported that metal-free carbon materials with high specific surface areas and porous structures generally have high

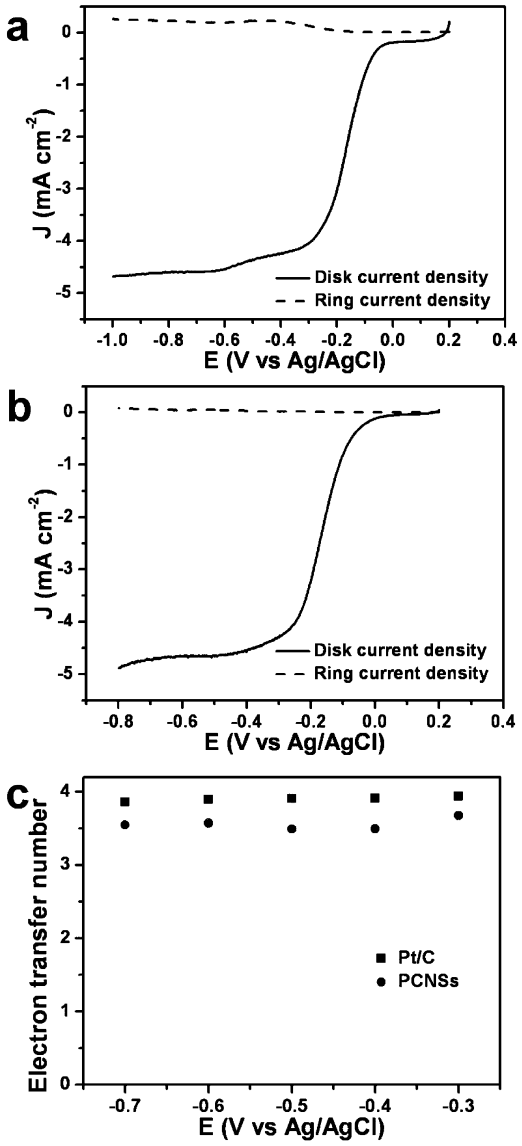

Figure 6. RRDE determination of (a) PCNSs/GCE and (b) Pt/C/GCE in N_2- or O_2-saturated 0.1 M KOH at a scan rate of 10 mV s^{-1}. (c) Numbers of electrons transferred for the ORR.

limiting current densities compared with the Pt/C. The high limiting current density in PCNSs may be due to its large specific surface area and porous nature, which provides a large electrolyte-accessible surface area to enhance the utilization of nitrogen active sites and proper channels for mass diffusion, leading to a much higher electrochemical activity.[24,36]

Besides the potential and electron-transfer number, stability is another important property that should be studied in alkaline-fuel-cell technology. We used the chronoamperometric method to investigate the stability of PCNSs as the catalyst of the ORR. Figure 7 shows the current−time curves of the PCNSs/GCE and the Pt/C/GCE at a constant potential of −0.4 V (vs Ag/AgCl) in a 0.1 M KOH solution saturated with O_2 at a rotation rate of 1600 rpm. The current at the PCNSs/GCE (gray line) shows a much slower attenuation than that at the Pt/C/GCE (black line). At the end of the determination, the ORR current loses 42.2% of its initial current value at the Pt/C/GCE (from 0.481 to 0.278 mA), whereas the current only loses 28.8% at the PCNSs/GCE (from 0.452 to 0.322 mA). Impressively, during the whole process, the current at the PCNSs/GCE decays at the same pace without any sharp decline, whereas Pt/C/GCE has an obvious decrease at the initial time. This phenomenon indicates that PCNSs possess better stability as the catalyst of the ORR.

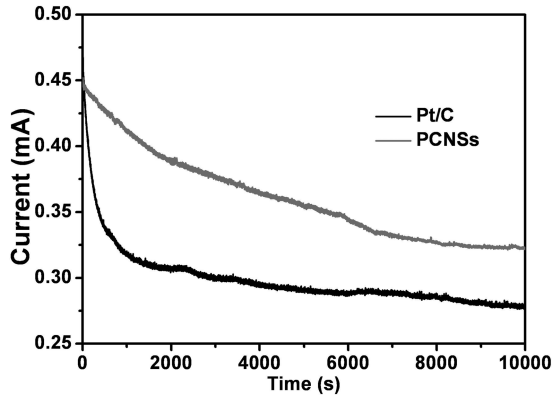

Figure 7. Chronoamperometric curves of PCNSs/GCE and Pt/C/GCE at −0.4 V in an O_2-saturated 0.1 M KOH solution at a rotation rate of 1600 rpm.

4. CONCLUSIONS

We developed a facile and green method to synthesize novel porous carbon nanosheets in the absence of any templates. The as-prepared nanomaterials have the properties of a large specific surface area and a large number of micropores and mesopores. Furthermore, the nanosheets exhibited excellent catalytic activity toward the ORR, high methanol tolerance, and good stability in comparison with the 20% commercial Pt/C catalyst in the alkaline solution. Depending on these physical and chemical properties, the prepared porous materials might have potential uses in applications for supercapacitors and supporters. In addition, it is expected that this study will provide inspiration for preparing carbon materials by a bottom-up approach.

AUTHOR INFORMATION

Corresponding Author

*Tel.: +86 431 85262426; Fax: +86 431 85685653; E-mail: jiangxiue@ciac.jl.cn.

Notes

The authors declare no competing financial interest.

ACKNOWLEDGMENTS

This work was supported by the Natural Science Foundation of Jilin Province (201215092), President Funds of the Chinese Academy of Sciences, and the Youth Foundation of China (21105097).

REFERENCES

(1) Steele, B. C. H.; Heinzel, A. *Nature* **2001**, *414*, 345−352.
(2) Levendorf, M. P.; Kim, C.-J.; Brown, L.; Huang, P. Y.; Havener, R. W.; Muller, D. A.; Park, J. *Nature* **2012**, *488*, 627−632.
(3) Xiao, L.; Zhuang, L.; Liu, Y.; Lu, J.; Abruna, H. D. *J. Am. Chem. Soc.* **2008**, *131*, 602−608.
(4) Gong, K.; Du, F.; Xia, Z.; Durstock, M.; Dai, L. *Science* **2009**, *323*, 760−764.
(5) Wang, S.; Yu, D.; Dai, L.; Chang, D. W.; Baek, J.-B. *ACS Nano* **2011**, *5*, 6202−6209.

(6) Stamenkovic, V. R.; Fowler, B.; Mun, B. S.; Wang, G.; Ross, P. N.; Lucas, C. A.; Marković, N. M. *Science* **2007**, *315*, 493−497.
(7) Henry, J. B.; Maljusch, A.; Huang, M.; Schuhmann, W.; Bondarenko, A. S. *ACS Catal.* **2012**, *2*, 1457−1460.
(8) Lee, C.-L.; Chiou, H.-P.; Syu, C.-M.; Wu, C.-C. *Electrochem. Commun.* **2010**, *12*, 1609−1613.
(9) Yin, H.; Tang, H.; Wang, D.; Gao, Y.; Tang, Z. *ACS Nano* **2012**, *6*, 8288−8297.
(10) Guo, S.; Zhang, S.; Wu, L.; Sun, S. *Angew. Chem., Int. Ed.* **2012**, *51*, 11770−11773.
(11) Wen, Z.; Ci, S.; Zhang, F.; Feng, X.; Cui, S.; Mao, S.; Luo, S.; He, Z.; Chen, J. *Adv. Mater.* **2012**, *24*, 1399−1404.
(12) Liu, R.; Wu, D.; Feng, X.; Müllen, K. *Angew. Chem., Int. Ed.* **2010**, *49*, 2565−2569.
(13) Zhao, Y.; Hu, C.; Hu, Y.; Cheng, H.; Shi, G.; Qu, L. *Angew. Chem., Int. Ed.* **2012**, *51*, 11371−11375.
(14) Liang, J.; Jiao, Y.; Jaroniec, M.; Qiao, S. Z. *Angew. Chem., Int. Ed.* **2012**, *51*, 11496−11500.
(15) Chen, S.; Bi, J.; Zhao, Y.; Yang, L.; Zhang, C.; Ma, Y.; Wu, Q.; Wang, X.; Hu, Z. *Adv. Mater.* **2012**, *24*, 5593−5597.
(16) Qu, L.; Liu, Y.; Baek, J.-B.; Dai, L. *ACS Nano* **2010**, *4*, 1321−1326.
(17) Kundu, S.; Nagaiah, T. C.; Xia, W.; Wang, Y.; Dommele, S. V.; Bitter, J. H.; Santa, M.; Grundmeier, G.; Bron, M.; Schuhmann, W.; Muhler, M. *J. Phys. Chem. C* **2009**, *113*, 14302−14310.
(18) Yang, L.; Jiang, S.; Zhao, Y.; Zhu, L.; Chen, S.; Wang, X.; Wu, Q.; Ma, J.; Ma, Y.; Hu, Z. *Angew. Chem., Int. Ed.* **2011**, *50*, 7132−7135.
(19) Yang, D. S.; Bhattacharjya, D.; Inamdar, S.; Park, J.; Yu, J. S. *J. Am. Chem. Soc.* **2012**, *134*, 16127−16130.
(20) Jin, Z.; Nie, H.; Yang, Z.; Zhang, J.; Liu, Z.; Xu, X.; Huang, S. *Nanoscale* **2012**, *4*, 6455−6460.
(21) Zheng, Y.; Jiao, Y.; Ge, L.; Jaroniec, M.; Qiao, S. Z. *Angew. Chem., Int. Ed.* **2013**, *52*, 3110−3116.
(22) Chen, X.; Wu, G.; Chen, J.; Chen, X.; Xie, Z.; Wang, X. *J. Am. Chem. Soc.* **2011**, *133*, 3693−3695.
(23) Yang, S.; Feng, X.; Wang, X.; Müllen, K. *Angew. Chem., Int. Ed.* **2011**, *50*, 5339−5343.
(24) Pachfule, P.; Dhavale, V. M.; Kandambeth, S.; Kurungot, S.; Banerjee, R. *Chem.—Eur. J.* **2013**, *19*, 974−980.
(25) Liu, G.; Li, X.; Ganesan, P.; Popov, B. N. *Appl. Catal., B* **2009**, *93*, 156−165.
(26) Chen, L. F.; Zhang, X. D.; Liang, H. W.; Kong, M.; Guan, Q. F.; Chen, P.; Wu, Z. Y.; Yu, S. H. *ACS Nano* **2012**, *6*, 7092−7102.
(27) Yu, D.; Wei, L.; Jiang, W.; Wang, H.; Sun, B.; Zhang, Q.; Goh, K.; Si, R.; Chen, Y. *Nanoscale* **2013**, *5*, 3457−3464.
(28) Dresselhaus, M. S.; Jorio, A.; Hofmann, M.; Dresselhaus, G.; Saito, R. *Nano Lett.* **2010**, *10*, 751−758.
(29) Zhou, Y.; Bao, Q.; Tang, L. A. L.; Zhong, Y.; Loh, K. P. *Chem. Mater.* **2009**, *21*, 2950−2956.
(30) Ming, H.; Pan, K.; Liu, Y.; Li, H.; He, X.; Ming, J.; Ma, Z.; Kang, Z. *J. Cryst. Growth* **2011**, *327*, 251−257.
(31) Li, Y.; Zhao, Y.; Cheng, H.; Hu, Y.; Shi, G.; Dai, L.; Qu, L. *J. Am. Chem. Soc.* **2012**, *134*, 15−18.
(32) Ahmed, M. S.; Jeon, S. *J. Power Sources* **2012**, *218*, 168−173.
(33) Lu, Y.; Wang, Y.; Chen, W. *J. Power Sources* **2011**, *196*, 3033−3038.
(34) Lu, J.; Bo, X.; Wang, H.; Guo, L. *Electrochim. Acta* **2013**, *108*, 10−16.
(35) Chen, P.; Xiao, T. Y.; Qian, Y. H.; Li, S. S.; Yu, S. H. *Adv. Mater.* **2013**, *25*, 3192−3196.
(36) Yang, W.; Fellinger, T.-P.; Antonietti, M. *J. Am. Chem. Soc.* **2010**, *133*, 206−209.